Electron and hole polaron asymmetry in a two-band Peierls-Hubbard material

J. Tinka Gammel, R. J. Donohoe, A. R. Bishop, and B. I. Swanson

Isotope and Nuclear Chemistry and Theoretical Divisions, and Centers for Materials Science and Nonlinear Studies,
Los Alamos National Laboratory, Los Alamos, New Mexico 87545
(Received 4 June 1990)

A combined experimental and theoretical analysis of the quasi-one-dimensional mixed-valence insulator $[Pt(en)_2][Pt(en)_2Cl_2] \cdot (ClO_4)_4$ ($en = N_2C_2H_8$) is given. Three intragap absorptions, observed directly by near- and mid-infrared single-crystal transmission experiments and indirectly by resonance-Raman excitation profiles, can be *quantitatively* accounted for with an extended Peierls-Hubbard chain model incorporating $\frac{3}{4}$-filling of two bands, with striking asymmetry between electron and hole polarons. Analogies are drawn to modeling other strong-correlation novel materials, including oxide superconductors.

The physics of narrow-band strongly correlated insulators, and their pressure-, photoexcitation-, and doping-induced intragap states continues to attract considerable interest, especially in low-dimensional (D) materials such as charge-transfer salts, conducting polymers, and oxide superconductors. Strong competitions for broken-symmetry ground state are controlled by electron-phonon (e-ph) and electron-electron (e-e) interactions and by dimensionality. These factors need to be understood theoretically, and tuned experimentally, if the "novel" states of matter are to be utilized efficiently for special-purpose materials. Here we report on a successful integrated making-measuring-modeling approach to a class of materials of this type: *ab initio* and band-structure input to a many-body Peierls-Hubbard Hamiltonian has yielded *quantitative* agreement with ground- and excited-state experimental data.

The large *class* of materials[1] having the form of halogen-bridged transition-metal linear-chain complexes (*MX* chain complexes; *M*, metal, *X*, halogen) offers an exciting possibility to systematically vary the competing forces through a very large range of single-crystal materials—using pressure, doping, and chemical variations of *M*, *X*, and the ligand structure. The ligands are attached to the metals and hold the chains of alternating *M* and *X* into anisotropic three-dimensional (3D) structures. Thus, PtCl (i.e., *M*=Pt, *X*=Cl) compounds typically[1] have a ground state in which a large-amplitude dimerization of the Cl sublattice displacements is stabilized by an equally strong-valence dimerization on the Pt sublattice. The strength of this charge-density-wave (CDW) distortion decreases as *X* is replaced with Br and I toward the valence delocalized (weak-distortion) regime.[2] Indeed Pt_2Br (based on the *MMX* monomer) under pressure[3] and NiBr (Ref. 4) are undimerized, and a spin-density-wave (SDW) ground state probably occurs.

Tuning through the transition regions between ground states is especially interesting, as seen in recent studies of high-temperature superconducting oxides.[5] In fact, the *MX* class has much in common with current modeling of oxide superconductors. At stoichiometry, both are nominally $\frac{3}{4}$-filled, hybridized two-band materials in which both e-e and e-ph interactions are important, described by similar model Hamiltonians—the similarity with $Ba_{1-x}Pb_xBiO_3$ is especially direct.[6] This analogy extends to electron or hole *doping* of the broken-symmetry ground states leading to discussion of polarons, bipolarons, excitons, and domain walls as self-trapped local defect states (bags).

In this work we report results for $[Pt(en)_2][Pt(en)Cl_2](ClO_4)_4$ (hereafter referred to as PtCl; $en = N_2C_2H_8$). Early experimental studies of polaron states in *MX* materials focused on high-energy intragap absorption features ("*A*" and "*B*" bands).[7] We now find these to be accompanied by a much lower-energy ("*C*") band.[8] We argue that resonant Raman (RR) profiles resolve the *A* and *B* bands into *distinct* absorptions for electron and hole polarons. Direct comparisons between experiment and theory show (i) a 1D extended Peierls-Hubbard model Hamiltonian with $\frac{3}{4}$-filling of two bands is in *quantitative* agreement with experiment, (ii) photoexcitation above the intervalence charge-transfer (IVCT) band-gap results in localized electron and hole polarons, and (iii) *asymmetry* exists between electron and hole polarons in terms of both their characteristic vibrational modes and their intragap absorption transitions. Previous theoretical studies[6,9,10] focused on approximate $\frac{1}{2}$-filled *one-band* models which do not exhibit this asymmetry. The importance of electron-hole asymmetry has also been suggested in recent studies of quasi-2D oxide superconductors.[11]

Synthesis of PtCl was achieved using previously reported methods.[12] Infrared (ir) transmission difference spectra of oriented single crystals obtained before and after photoexcitation into the IVCT band at 20 K (Ref. 8) show the growth of a new feature ca. 3200 cm^{-1} (*C* band). The increase in intensity of this new feature, eventual saturation at long photolysis times, and decay upon warming the sample to room temperature all correlate with the behavior of the *A* and *B* bands. It has not been possible to obtain transmission spectra in the *A* and *B*

and the C regions simultaneously. However, separate experiments on crystals with the same approximate thickness indicate that the C-band intensity is significantly less than that of the A and B bands; the *relative* intensities estimated from observed absorbences are depicted in Fig. 1. We attribute these intragap features to polarons as (1) they grow in and decay at the same rate as paramagnetic defects observed in EPR, (2) the energies of the A, B, and, in particular, the mid-IR (C) bands can only be consistent with polaronic defects, and (3) the energies, intensities, and line shapes of the intragap absorptions *quantitatively* agree with calculations using polarons (see below).

RR spectra polarized along the chain axis of single crystals held at 15 K were obtained using excitation energies varying from 1.2 to 2.5 eV. Defect states in the as-grown crystals were studied by tuning the excitation energy from the red[13] towards the IVCT band edge in order to avoid complications from metastable photoexcited states. Photoinduced defect states were studied using a probe beam to the red of the IVCT after photoexcitation into the IVCT. Focused laser intensity at the sample was, in all cases, less than 5 mW. Further experimental details are given elsewhere.[14,15] Vibrational features were observed about 287, 272, and 263 cm^{-1}.

RR studies of crystals before photoexcitation into the IVCT show evidence for weak vibrational modes that can be attributed to defect states.[14] Here we focus on the features about 287 and 263 cm^{-1}. RR experiments performed using excitation to the red of the A band (1.3–1.5 eV) before and after photoexcitation into the IVCT transition show that both the 287- and 263-cm^{-1} features show the same growth and decay rates as the A, B, and C bands.[16] Accordingly, we attribute them to local modes of polarons. On the basis of expected[17] changes in the Pt-Cl force constants upon oxidation of Pt II (hole) versus reduction of Pt IV (electron) sites, we attribute the vibrations at 287 and 263 cm^{-1} to hole and electron polarons, respectively. The feature at 287 cm^{-1} exhibits two distinct regions of enhancement centered slightly to the red of the A band (1.4–1.7 eV) and slightly to the red of
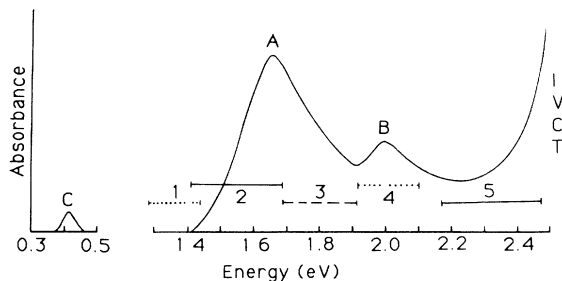

FIG. 1. Intragap optical absorption features for $[Pt(en)_2][Pt(en)_2Cl_2]\cdot(ClO_4)_4$ with RR enhancement regions (1–5) superimposed. The RR data separates the optical data into distinct features for electron (regions 1 and 4—dotted—enhancing a phonon at 263 cm^{-1}) and hole (regions 2 and 5—solid—enhancing phonon at 287 cm^{-1}) polarons. Region 3—dashed—enhances a phonon a 272 cm^{-1} (see text).

the IVCT band edge (2.17–2.5 eV). In contrast, the broader RR feature at 263 cm^{-1} is enhanced in a region further to the red of the A band (1.28–1.43 eV) and in the region corresponding to the B band (1.92–2.1 eV). These distinct enhancement regions are also depicted in Fig. 1.

Turning to our theoretical modeling, we consider an isolated MX chain. Focusing on the metal d_{z^2} and halogen p_z orbitals and including only near-neighbor interactions, we use the following two-band tight-binding many-body Hamiltonian:[18]

$$H = \sum_{l,\sigma} \{ (-t_0 + \alpha\Delta_l)(c_{l,\sigma}^\dagger c_{l+1,\sigma} + c_{l+1,\sigma}^\dagger c_{l,\sigma})$$
$$+ [(-1)^l e_0 - \beta_l(\Delta_l + \Delta_{l-1})]c_{l,\sigma}^\dagger c_{l,\sigma}\}$$
$$+ \sum_l U_l n_{l\uparrow} n_{l\downarrow} + \tfrac{1}{2}K \sum_l \Delta_l^2$$
$$+ \tfrac{1}{2}K_{MM} \sum_l (\Delta_{2l} + \Delta_{2l+1})^2 . \tag{1}$$

M and X atoms occupy even and odd sites, respectively. Δ_l is the deviation from uniform lattice spacing between sites l and $l+1$. Here parameters are the difference between M and X electron affinities ($2e_0 = \varepsilon_M - \varepsilon_X$), electron hopping ($t_0$), on-site[19] ($\beta_M, \beta_X$) and intersite ($\alpha$) *e-ph* coupling, on-site *e-e* repulsion (U_M, U_X), and finally effective M-X (K) and M-M (K_{MM}) springs to model the elements of the structure not explicitly included: K_{MM} accounts for the rigidity of the M (plus ligands) sublattice. Since photoinduced defects have the same experimental spectra as those in the dark, we have not chosen to model trapping on preexisting defects.

The general model is capable of supporting several ground states:[18] period-4 CDW, SDW, bond-order-wave (BOW), spin-Peierls, as well as intriguing long-period (superlattice) patterns.[20] For PtCl, a combination of ground-state experimental data [the Cl sublattice distortion amplitude (0.38 Å), the $\sigma(Cl) \rightarrow d\sigma^*$ absorption for the oxidized monomer (4.7 eV), and the IVCT band edge (2.5 eV)] and quantum chemical calculations[21] on small PtCl clusters (including ligands), appropriate to the highly valence localized limit, lead us to the following Hartree-Fock (HF) effective ($U = 0$) parameter set for the Hamiltonian (1): $t_0 = 1.6$ eV, $\alpha = 2.4$ eV/Å, $e_0 = 0.96$ eV, $\beta_M = 0.16$ eV/Å, $K = 3.9$ eV/Å^2, and $K_{MM} = \infty$. For $K_{MM} \gtrsim K$ our results are insensitive to K_{MM} and β_X. For $U \neq 0$, these values must be adjusted so that the same uniform band structure results. For small to intermediate U, agreement of exact diagonalization and HF or perturbation theory is excellent (for both ground- and defect-state structure and optical absorption). This is a consequence of the $\tfrac{3}{4}$-filling in a CDW regime and is to be contrasted with the discussion of $\tfrac{1}{2}$-filled one-band models, where true *e-e* correlation effects dominate. We anticipate $U \sim 1$–2 eV in PtCl.

Figure 2 shows the optical absorptions predicted for hole and electron polarons and bipolarons calculated on a 100-site chain with one or two electrons added or subtracted from $\tfrac{3}{4}$-filling. The combined electron-lattice Hamiltonian was allowed to relax (adiabatically) to the new ground state and the absorption was calculated from
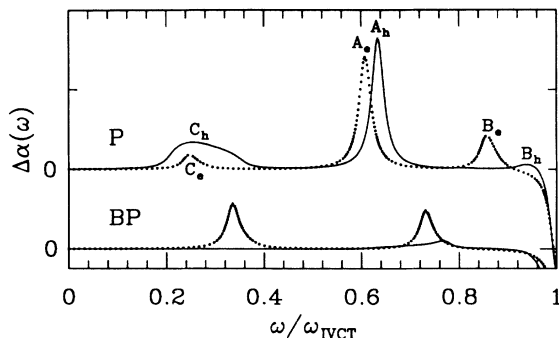
FIG. 2. Optical absorption spectra, with the IVCT scaled to unity and uniform absorption subtracted, for the electron (dotted) and hole (solid) polaron (P) and bipolaron (BP) (PtCl parameters). Note the electron-hole asymmetry.

FIG. 3. Lattice positions of the metal ($\bigcirc$) and halogen ($\Diamond$, displacement exaggerated by a factor of 2 for clarity), excess charge density (solid line), and the excess spin density (dotted line) for the defects of Fig. 2. Note the electron-hole asymmetry.

the Golden Rule—the results were Lorentzian smoothed, but no inhomogeneous broadening was included. We find three distinct intragap[13] absorption features for each polaron species and one and two intragap features for the hole and electron bipolarons, respectively. Corresponding results have been obtained for negatively charged, positively charged, and neutral kinks, and for excitons, as described elsewhere.[18] Figure 3 shows the associated local lattice distortions and charge distributions. Note the X sublattice distortion follows the CDW on the M's, and for the bipolarons the lattice distortion is 180° out of phase at the bipolaron center. While all defects are highly localized structural distortions (consistent with the valence localized ground state), the charge distortion is significantly shared with neighboring atoms only for the *hole* defects. EPR experiments[22] suggest the spin density is spread over approximately two Pt sites. We also remark that the defects are accompanied (for $K_{MM} \neq \infty$) by a small local BOW (M sublattice) distortion even though the ground state is purely CDW.

Comparing Figs. 1 and 2, we conclude that the agreement is excellent and supports the interpretation of hole-polaron absorptions at $A_h \simeq 1.5$ eV and $B_h \simeq 2.3$ eV (RR profiles 2 and 5, enhancing the vibration at 287 cm^{-1}), with electron-polaron absorption at $A_e \simeq 1.3$ eV, $B_e \simeq 2.0$ eV, and $C_e \simeq 0.4$ eV (RR profiles 1 and 4, enhancing the *softer* vibration at 263 cm^{-1}). The predicted C_h structure is too broad to be detected by the experimental technique used here and will need an alternative experimental probe. The A band observed to grow in upon photoexcitation corresponds to hole and electron polarons with the electron polarons contributing to the red edge of this intragap transition. Further, the B band is dominated by the electron polaron while the expected B_h absorption is within, and unresolved from the IVCT band edge. Single-crystal transmission experiments[7,8] have shown no evidence for a resolved A-band feature for the electron polaron, although this is a difficult region owing to poor instrument response. Our RR results are important in that they demonstrate that electron and hole polarons have distinct vibrational modes which, in turn, have distinct excitation profiles.

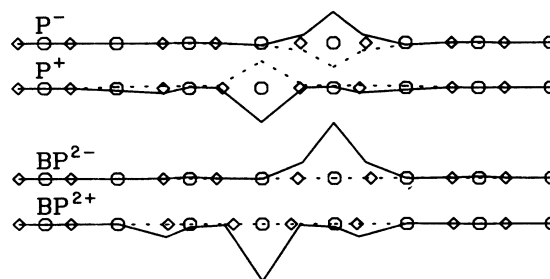Although our theoretical treatment has centered on self-trapped electron and hole polarons on an otherwise undistorted chain, several experimental details, such as the EPR signal[22] and long lifetimes of photoinduced polaronic states, suggest trapping on preexisting defects (such as adjacent reduced metal centers). Preliminary studies show that weak pinning potentials do not affect the calculated A-, B-, and C-band absorptions—in particular the asymmetry—significantly. More detailed experimental and theoretical studies are underway.

The assignment of the peak observed at 272 cm^{-1}, enhanced in region 3, is not yet clear. Although this absorption region coincides with that predicted for electron bipolarons (see Fig. 2), lattice dynamics calculations do not support this assignment.[17] Rather, the electron bipolaron should yield a Raman-active phonon that is lower in energy than the electron polaron mode at 263 cm^{-1}. However, preliminary studies of the temperature dependence of the MX chain defect phonons show that, upon warming from 12 K, the signal at 272 cm^{-1} is diminished, while the signal at 263 cm^{-1} gains intensity. This suggests that the 272-cm^{-1} phonon is due to an unidentified defect that is converted into electron polarons upon warming.

In conclusion, we have demonstrated the validity of an extended Peierls-Hubbard, $\frac{3}{4}$-filled, two-band model for isolated chains of $[Pt(en)_2][Pt(en)_2Cl_2](ClO_4)_4$. We have shown that model parameter values extracted from quantum chemical calculations and ground-state experimental data can *quantitatively* explain observed intragap absorptions. We stress that a $\frac{3}{4}$-filled, two-band model is *essential* in explaining the striking asymmetry observed between electron- and hole-polaron absorptions.[23] The lessons and techniques used here will be important in other MX materials and more generally in novel low-D materials with strong competitions for broken-symmetry ground states, including the analogous 2D and 3D oxide superconductors.[5]

[1]H. J. Keller, in *Extended Linear Chain Compounds,* edited by J. S. Miller (Plenum, New York, 1982), Vol. 1, p. 357.

[2]R. J. H. Clark, in *Advanced in Infrared and Raman Spectroscopy,* edited by R. J. H. Clark and R. E. Hester (Wiley Heyden, New York, 1984), Vol. 11, p. 95.

[3]B. I. Swanson, M. A. Stroud, S. D. Conradson, and M. H. Zeitlow, Solid State Commun. **65,** 1405 (1988).

[4]H. Toftlund and O. Simonsen, Inorg. Chem. **23,** 4261 (1984); K. Toriumi, Y. Wada, T. Mitani, and S. Bandow, J. Amer. Chem. Soc. **111,** 2341 (1989).

[5]For example, Proceedings of the IBM Europe Institute 1988 Workshop on High Temperature Superconductivity, Oberlech, Austria, 1988, edited by K. A. Mueller [IBM J. Res. Dev. **33** (1989)].

[6]D. Baeriswyl and A. R. Bishop, Phys. Scr. T **19,** 239 (1987); J. Phys. C **21,** 339 (1988); S. D. Conradson, M. A. Stroud, M. H. Zeitlow, B. I. Swanson, D. Baeriswyl, and A. R. Bishop, Solid State Commun. **65,** 723 (1988).

[7]S. Kurita, M. Haruki and K. Miyagawa, J. Phys. Soc. Jpn. **57,** 1789 (1988); L. Degiorgi, P. Wachter, M. Haruki, and S. Kurita, Phys. Rev. B **40,** 3285 (1989).

[8]R. J. Donohoe, S. A. Ekberg, C. D. Tait, and B. I. Swanson, Solid State Commun. **71,** 49 (1989).

[9]K. Nasu, J. Phys. Soc. Jpn. **50,** 235 (1981); **52,** 3865 (1983); **53,** 302 (1984); **53,** 427 (1984); **54,** 1933 (1985); A. Mishima and K. Nasu, Synth. Met. **29,** F175 (1989); Phys. Rev. B **40,** 5593 (1989).

[10]Y. Ichinose, Solid State Commun. **50,** 137 (1984); Y. Onodera, J. Phys. Soc. Jpn. **56,** 250 (1987).

[11]J. E. Hirsch and F. Marsigilio, Phys. Rev. B **39,** 11 515 (1989).

[12]F. Basolo, J. C. Bailar, Jr., and B. R. Tarr, J. Am. Chem. Soc. **72,** 2433 (1950).

[13]We limit the theoretical discussion here to intragap features. Features predicted and observed to the blue of the IVCT are planned to be discussed elsewhere. (See Refs. 15 and 18.)

[14]R. J. Donohoe, C. D. Tait, and B. I. Swanson, Chem. Mater. **2,** 315 (1990).

[15]B. I. Swanson, R. J. Donohoe, L. A. Worl, A. D. F. Bulou, C. Arrington, J. T. Gammel, A. Saxena, and A. R. Bishop, Proceedings from the Symposium on Photoinduced Electron Transfer, Rochester, New York, 1990 [Mol. Cryst. Liq. Cryst. (to be published)]; B. I. Swanson, R. J. Donohue, L. A. Worl, J. T. Gammel, A. Saxena, I. Batistic, and A. R. Bishop, Synth. Met. (to be published).

[16]R. J. Donohoe, R. B. Dyer, and B. I. Swanson, Solid State Commun. **73,** 521 (1990).

[17]Reduction of Pt IV to form Pt III should result in a larger decrease in the Pt-Cl stretching force constant and a lower vibrational frequency for the local gap state than oxidation of Pt II. A. D. F. Bulou, R. J. Donohoe, and B. I. Swanson (unpublished).

[18]A. R. Bishop, J. T. Gammel, and S. R. Phillpot, Synth. Met. **29,** F151 (1989).

[19]In the Hartree-Fock approximation the Hubbard terms (U_M, U_X, V) have the same (disproportionation) effect on the band structure and lattice distortion as the on-site e-ph interaction (β_M, β_X). Both mechanisms— $V > U$ [e.g., C. M. Varma, Phys. Rev. Lett. **61,** 2713 (1988)] and on-site e-ph coupling [e.g., T. M. Rice and L. Sneddon, *ibid.* **47,** 689 (1981)]—have been proposed to drive the CDW in $Ba_{1-x}Pb_xBiO$ and both yield effective "negative-U" models. Similar choices may exist in the MX chain compounds.

[20]I. Batistic, A. R. Bishop, and J. T. Gammel, Synth. Met. (to be published).

[21]R. L. Martin and P. J. Hay (unpublished).

[22]A. Kawamori, R. Aoki, and M. Yamashita, J. Phys. **18,** 5487 (1985).

[23]The $\frac{1}{2}$-filled, two-band case (AB polymer) has an asymmetry in the levels about midgap, but the absorptions predicted for electron and hole polarons are the same.